Characterization of Plasma Activated Water for Medical Applications

P.S Ganesh Subramanian*, R. Harsha, D.K. Manju, M. Hemanth, R. Lakshminarayana, M.S. Anand, S. Dasappa

Indian Institute of Science, Bangalore, Karnataka, India

*Corresponding author: E-mail: psgs123xyz@gmail.com

Abstract

Non-thermal plasma discharge in air generates several species, including reactive oxygen and nitrogen species (RONS). If, plasma is generated above a water column, some of these species gets transferred into the water column below generating plasma activated water (PAW), which is known to have several applications. These applications are attributed to the reactive species generated by the plasma discharge. To cater specifically to each application, a complete chemical characterization of plasma discharge in air and PAW is vital, as each of these species have their own unique contribution to the application of PAW. In this work, analysis of the plasma discharge in air using optical emission spectroscopy (OES) and detailed characterization of PAW for its chemical constituents was done. In PAW, the parameters namely, pH, electrical conductivity (EC), H_2O_2, NO_3^-, and NO_2^- were quantified as a function of plasma exposure time. The values of NO_3^- (6000 μM) and EC (4600 μS) obtained in this study were about 50% and 130% higher respectively, than what has generally been reported. The antimicrobial nature of the PAW on Pseudomonas *aeruginosa,* one of the bacteria responsible for nosocomial infections was also tested, and PAW was able to inactivate the bacterium. Copyright © VBRI Press.

Keywords: Plasma activated water, nitrate, nitrite, hydrogen peroxide, dielectric barrier discharge plasma, pseudomonas. aeruginosa.

Introduction

Plasma is one of the four fundamental states of matter first identified by Crookes in 1879. Subsequently, to explain electrical discharges in gases, Irving Langmuir coined the term plasma in 1928 [1]. Plasma is an electrically conducting gas. Any gas can be converted to a plasma state in two ways, either by applying a high potential difference between two metallic electrodes separated by a distance or by exposing the gas to extremely high temperatures, both leading to ionization of the gas. This ionization converts the otherwise non conducting gas into an electrically conducting state termed as a Plasma state. The former method of generating plasma under near room temperatures using high voltage/ high frequency power supplies is generally termed as "Cold Plasma" and has several applications.

Plasma state is composed of charged particles (electrons, positively and negatively charged ions), excited atoms & molecules, radicals, meta-stables and UV photons [2]. Some of the reported applications of plasma include low-temperature plasma activated bonding to obtain superior bond strength, plasma spraying, plasma arc melting for higher grade purification [3-8], ozonation, waste water treatment and hydrocarbon re-forming [9-14].When air plasma is created over a water column, some of the plasma species formed in the headspace above the water column, gets transported into the water column and the water becomes activated. This water is called plasma treated water or plasma activated water (PAW), which is known to have some unique properties and applications [15, 16]. The plasma treatment of water changes its chemical composition leading to acidification, and formation of reactive oxygen (ROS) and reactive nitrogen (RNS) species in PAW. The extent of acidification, concentration of ROS and RNS whose concentration depends on a variety of parameters such as plasma discharge type, the discharge power density, plasma volume formed, electrodes used, activation time, starting water chemistry and water volume. The generated ROS and RNS species, coupled with the pH of the PAW formed are responsible for unique applications of PAW [17].

In the last 15 years, a lot of study has been done to see the disinfection capabilities and anti-microbial efficacy of PAW on different microbes. Researchers have shown that the PAW can inactivate a wide range of microorganisms like bacteria, fungi, biofilms, viruses and spores [18-20]. Researchers have shown that, treatment with PAW leads to morphological changes in these micro-organisms [21]. The loss in membrane integrity reported, is believed to be caused by the generation of ROS and the resulting lipid peroxidation,

showing that the whole cell wall of the bacteria breaks down after treatment with PAW [**22**]. In addition to these antimicrobial properties, PAW has also been investigated for its promising application in anti-cancer therapy [**23, 24**].

The ROS and RNS present in the PAW is known to uniquely contribute towards its application, thereby making their quantification vital for understanding the scope and type of application PAW can have. As mentioned above, H_2O_2 and other ROS are responsible for the anti-bacterial and anti-cancer applications of PAW [**22**], while NO_3^- & NO_2^- are good nitrogen sources for the enhancement of germination and plant growth application [**17**].

In this study, an attempt has been made to characterize the PAW for ROS and RNS formed. This study also shows the antimicrobial nature of the PAW against *Pseudomonas aeruginosa* (*P. aeruginosa)* which is an opportunistic, multidrug resistant bacterium that targets the immunocompromised patients. and is one of the bacteria responsible for nosocomial infections. Similar work i.e., use of PAW for antimicrobial applications, has been published on the medical applications of plasma by Laurita *et al.* [**25**], but the work presented here reports the anti-microbial efficacy of PAW against P. aeruginosa. Electrical conductivity and NO_3^- values obtained in this study are about 130% and 50% higher respectively, than what has generally been reported. The details are presented below.

Experimental

PAW generation and its device

Fig. 1 shows a schematic representation of the device used to generated PAW. The device consisted of a 1 L borosilicate glass bottle which was used to hold the water to be activated. Metallic electrodes (diameter $= 0.9 \pm 0.1\ mm$, length $= 1.1 \pm 0.1\ m$) separated by a dielectric (silicone insulation $= 1.5\ mm$ thick) served as plasma forming electrodes. As shown in **Fig. 1**, the whole electrode setup was attached to the cap of the borosilicate glass jar. A 4 kV HV-AC power supply with an output frequency of 20 kHz was used as plasma power supply.
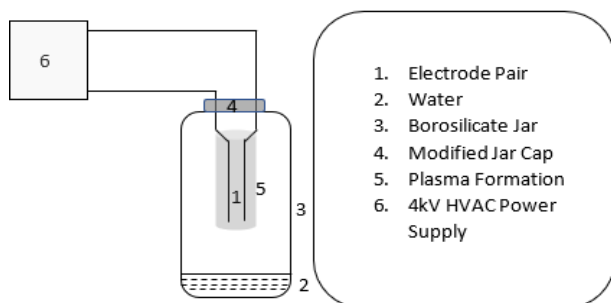

1. Electrode Pair
2. Water
3. Borosilicate Jar
4. Modified Jar Cap
5. Plasma Formation
6. 4kV HVAC Power Supply

Fig. 1. Schematic Diagram of the PAW generation device.

To activate water, $20\ ml$ of Millipore water was added to the borosilicate jar which was then closed with the cap containing the electrodes. The plasma power supply was switched ON for the desired activation time i.e., $3, 6, 9, 12$ and 18 minutes. At the end of the activation time, the power supply was turned OFF and the cap with the electrodes was removed and replaced with a normal cap. The contents of the jar were then well shaken for a minute to ensure mixing of the activated air and water.

Measurement of PAW parameters

The parameters that were characterized in PAW were Electrical Conductivity (EC), pH, & concentrations of Hydrogen Peroxide (H_2O_2), Nitrate (NO_3^-) and Nitrite (NO_2^-) ions.

The EC was measured using a conductivity meter (Aquasol EC/TDS meter AM-P-EC, E715044) with an accuracy of $1\ \mu S\ /cm$ in the range 1 to 9999 $\mu S\ /cm$. The pH was measured using a pH electrode (Thermo-Fischer Orion Ross Sure-Flow pH Electrode – 8172BNWP) with an accuracy of 0.01. The NO_3^- concentration was measured, using spectrophotometry at $500\ nm$ as per modified cadmium reduction method procedure [**26**]. The NO_2^- concentration was measured using diazotization method [**27**] at wavelength of $507\ nm$. The H_2O_2 concentration was measured using a semiquantitative Quantofix peroxide 25 and 100 strips (Macherey-Nagel, *Düren*).

Optical emission spectroscopy (OES) of the plasma discharge in the air was conducted using M/s Ocean optics HR4000 equipment with fiber optic sensor. This spectrometric system had an optical resolution of 0.02-8.4 nm full width half maximum (FWHM), wavelength range of 190 -1100 nm, 300 lines per mm grating density blazed and 5 μm slit width. The spectrometric parameters namely integration time and boxcar width were 5 s and 0 s, respectively.

Anti-Microbial efficacy of PAW on P. aeruginosa

The PAW was prepared by activating $20\ ml$ of Millipore water for 18 mins.

Using an inoculating loop, a culture of the *P. aeruginosa* was taken from an existing culture plate and spread onto two different plates containing a sheep blood agar media which was a differential media for the bacteria.

$1\ ml$ of PAW was added and spread on to one of the plates and $1\ ml$ of Millipore water was added on to the other plate which was used as a control. These plates were then incubated at $37^0\ C$ for 24 hours. After 24 hrs, these plates were examined for growth on *P. aeruginosa.*

Results and discussion

Characterization of PAW

Fig. 2 shows the variation of the EC values and the H+ ion concentration in the PAW for different activation time. The H+ ion concentration was calculated using pH values using the formula $[H^+] = 10^{-pH}$ in molarity units.
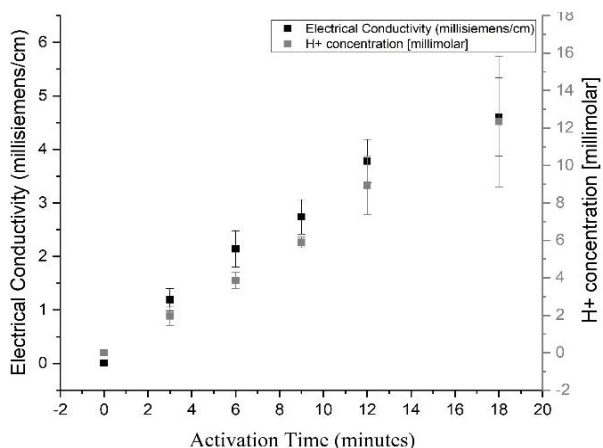
Fig. 2. Electrical Conductivity and Hydrogen ion concentration at different activation times.

As seen from **Fig. 2**, with increase in plasma activation time, both EC and H$^+$ ion concentration increase linearly with activation time. These parameters follow a linear trend as per the equations below where t_a is the plasma activation time in minutes and σ is the EC in mS/cm. From the equations, the fit is good.

$$\sigma = 0.255t_a + 0.368, R^2 = 0.97,$$
$$H+= 0.703t_a - 0.1246, R^2 = 0.99$$

This result is similar to the results reported by earlier studies in which, it has been shown that plasma activation of water leads to formation of H$^+$ ions in the water, forms RNS and ROS species and leads to the increase in EC [**25, 28**]. The plasma ionization leads to formation of NO_x in the air which when dissolved in water forms RNS, ROS and H+ ions in the water leading to acidification of water. The EC of the water also increases as the NO_3^- and NO_2^- ions formed in the water contribute positively, to increase the electrical conductivity of the water. The linear increase can be attributed to the fact that the power supplied in the plasma setup used was nearly constant throughout the activation time $(25.8 \pm 1.1\ W)$ and hence the concentration of H+ ions and EC also follow a linear trend.
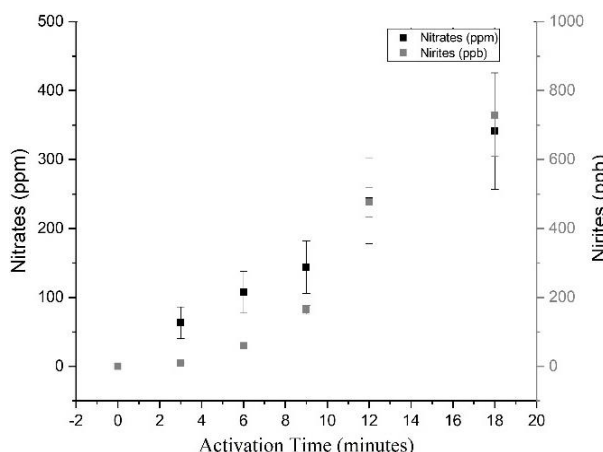

Fig. 3. Nitrate and Nitrite ion concentrations at different activation times.

Fig. 3 shows the NO_3^- and NO_2^- concentrations at different activation times. As observed from **Fig. 3**, with increase in activation time, both NO_3^- and NO_2^- ion concentrations increase. The NO_3^- concentration increases linearly with activation time whereas the NO_2^- ion does not follow a linear trend. The linearly regressed equation for the $[NO_3^-]$ is

$$NO_3^- = 19.008t_a - 2.876, R^2 = 0.99$$

The non-linear and delayed increase in NO_2^- concentrations may be attributed to NO_2^- being consumed to form some other species which reaches peak concentration around 3-6 minutes. One such species could be peroxinitrite which is formed by the reaction of H_2O_2 and NO_2^-, and has been reported to show anti-microbial properties [**16, 29**].

Fig. 4 shows H_2O_2 concentrations for different activation times. From **Fig. 4**, it is evident that, the H_2O_2 concentration increases with activation time, except for 18 mins of activation time, where a decrease was observed. This deviation from the increasing trend for the 18 mins activated PAW can be attributed to the pH interference associated with the measuring method. The quontofix tests strips are known to work well in the pH range of 2-9. The 18 mins activated PAW had a low pH of around 1.9 ± 0.1 and hence the observed trend. In order to verify this, buffer solutions ($NaHCO_3 - Na_2CO_3$) were activated with plasma and the H_2O_2 was measured. The plasma activated buffer solution (PABS)-after 18 min of activation showed higher H_2O_2 than PABS- 12 min of activation, as the pH was now was within the operational range of the test strips. These results are shown in **Fig. 4**.
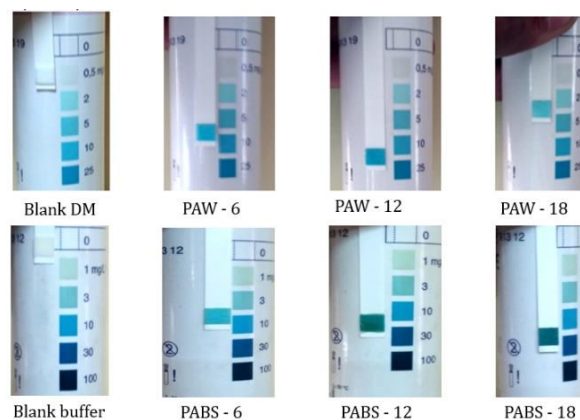

Fig. 4. Hydrogen Peroxide concentrations at different activation times.

Table 1, shows the the summary of reported PAW characterization parameters from literature, along with the results of this study. From **Table 1**, it is seen that the literature reports a variety of plasma sources to generate PAW i.e., DBD, jet and arc discharge, with varying plasma power, working volume and activation times. From **Table 1**, it is clear that the pH values obtained in this study are similar to the reported values. The EC values obtained in this study are higher values than those reported in earlier studies and is almost 130% and 190%

higher than the value reported by Vlad *et al.* [**30**] and Larita *et al.* [**25**] respectively. The NO_3^- values obtained in this study is 50% higher than those reported by Judee *et al.* [**31**]. The NO_2^- concentrations obtained in this study is lower than that reported by Xiang *et al.* [**32**]. These variations can be attributed to the variations in the plasma source, plasma power density, plasma volume formed and the activation times used.

Table 1. Chemical Characterization summary of the study compared with the literature.

Article	pH	EC $\mu S/cm$	H_2O_2 μM	NO_3^- μM	NO_2^- μM	Plasma Source	Activation Time (highest)	Plasma Power	Volume of water activated
Laurita Et al.[25]	2	1500-1600	250-280	3250-3500	80-100	Pulse DBD	10 *mins*		60 *ml*
Shen Et al.[28]	2.3		25	700	26	Jet	20 *mins*		10 *ml*
Chauvin Et al.[33]	4.3		1775	250	100	Jet	150 *s*		100 *μl*
Judee Et al.[31]	7.25	730	1870	3550	125	DBD	30 *mins*		50 *ml*
Xiang Et al.[32]	2.68	723	26.08	2000	1314	Jet	90 *s*	750 *W*	250 *ml*
Vlad Et al.[30]	1.8	1950	400	4300		Arc	50 *mins*	16 *W*	35 *ml*
This Study	1.9 ± 0.1	4600	300-750	6000	16	DBD	18 *mins*	25.8 $\pm 1.1\,W$	20 *ml*

Fig. 5 shows the optical emission spectra captured at different activation times. As shown in **Fig. 5**, several peaks were observed in the OES spectra. **Fig. 5a** shows the OES spectra which was captured right at the initiation of the activation and **Fig. 5b** shows the OES spectra at the end of 6 minutes of activation. From **Fig. 5**, it can also be noticed that, there is a difference in the peaks observed between 5a (0+ mins of activation) and 5b (6+ min of activation).
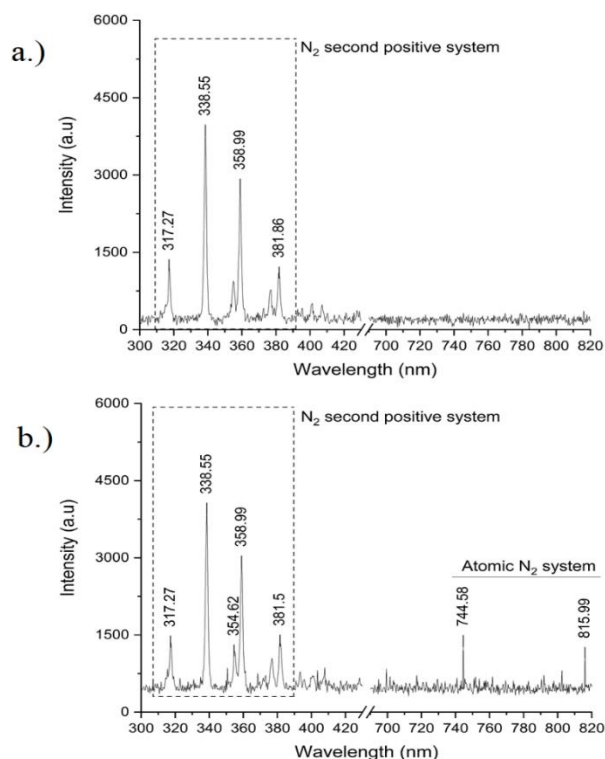

Fig. 5. (a) Optical emission spectra captured at the beginning of activation. (b) Optical emission spectra captured after 6 minutes of activation.

From **Fig. 5**, it can be seen that the prominent peaks of second positive system of Nitrogen between 315-400 nm range [**34-36**] were present at both activation times. However, the atomic nitrogen peaks at 744.3 nm and 818.3 nm were only observed at the 6 min activation time, indicating that extended activation leads to formation of atomic nitrogen in the PAW setup. The species at wavelength 337 nm and 358 nm are probably $N_2\ C^3\Pi_u$ or $NO\beta^3\Pi_g$ denoted (N_2/NO) [**34**]. It is hypothesized that, the prominence of the nitrogen peaks over the other peaks is responsible for the higher NO_3^- concentrations observed in this study relative to those reported before.

Fig. 6 shows the results of antimicrobial studies done on P. *aeruginosa*. **Fig. 6a** and **Fig. 6b** show the image of the control plate and PAW plate respectively, taken after 24 hours of incubation. From **Fig. 6**, it is clear that, there was no bacterial growth in the plate added with PAW whereas there were clear signs of bacterial growth on the control plate tested with DM water. This shows that that PAW shows antimicrobial efficacy on P. *aeruginosa*. This clearly indicates that PAW can be a potential solution to nosocomial diseases. There is also a lot of scope to use PAW for surface disinfection and sterilization which can be another medical application.
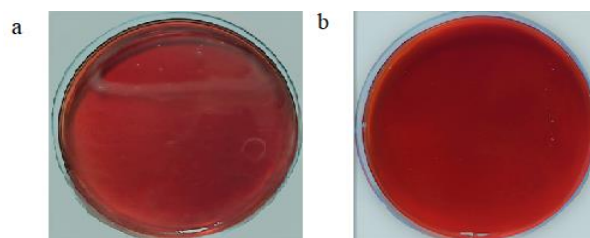

Fig. 6. (a) Control plate shows bacterial growth. (b) Plate added with PAW shows no bacterial growth.

A 5-day study was conducted to determine the potential of PAW to prevent microbial growth in nutrient media. The results showed that the plate onto which PAW was added had almost no microbial growth and was clean even after 5 days. Whereas, the control plates which were tested with de-ionized water had significant microbial growth, implying that the addition of PAW

onto surfaces can keep the surface free of bacteria for as long as 5 days.

Conclusion

This study reports a method of generating PAW using DBD discharge. The PAW generated was characterized for its ROS and RNS species and other parameters. All the chemical parameters measured in PAW showed an increasing trend with increase in activation time with many of them showing a linear trend with activation time. Electrical conductivity and NO_3^- concentration observed in this study were about 130% and 50% higher respectively, than what has been reported by others. The OES peaks were dominated by the second positive system of nitrogen.

This study also reports the antimicrobial nature of the PAW on P. *aeruginosa* and has the potential to be used to be used to prevent or reduce nosocomial infections.

Acknowledgements

Author's contributions

Ganesh Subramanian P S and Lakshminarayana R wrote the manuscript and designed the experiments. Ganesh Subramanian P S performed the experiments and interpreted the results. Harsha R, Hemanth M and Manju DK helped with the experiments. Lakshminarayana R, Dasappa S and Anand MS supervised the study, and provided the necessary experimental materials and facilities needed to conduct the experiments.

Conflicts of interest

The authors declare that they have no conflicts of interest.

References

1. Langmuir, I.; *Proc. Natl. Acad. Sci.,* **1928**.
2. Kalghatgi, S.; *et al. PLOS One,* **2011**, *6,* 1.
3. Elanski, D.; Mimura, K.; Ito, T.; Isshiki, M.; *Mater. Lett.*, **1997**, *30,* 1.
4. Dosta, S.; *et al. Appl. Catal. B Environ.,* **2016**, *189,* 151.
5. Carpio, P.; Candidato, R. T.; Pawłowski, L; Salvador, M. D.; *Surf. Coatings Technol.,* **2018**, *371,* 124.
6. Xu, J.; *et al. Appl. Surf. Sci.,* **2018**, *459,* 621.
7. He, R.; Yamauchi, A.; Suga, T.; *Jpn. J. Appl. Phys.,* **2018**, *57*.
8. Wang, C.; Wang, Y.; Tian, Y.; Wang, C.; Suga, T.; *Appl. Phys. Lett.,* **2017**, *110*.
9. J, A.; Rao, L.; Shivapuji, A. M.; & S, D; *Plasma Sources Sci. Technol.* In Press, **2019**.
10. Ananthanarasimhan, J.; Rao, L.; Shivapuji, A. M.; Dasappa, S.; Characterization and Applications of Non-Magnetic Rotating Gliding Arc Reactors - A Brief Review, **2019**, 31–38.
11. Ananthanarasimhan, J.; Rao, L.; Shivapuji, A. M.; Dasappa, S.; Observation of Arc Rotation and Voltage characteristics in Rotating Gliding Arc. Proc. ISPC, **2019**, *24,* 2.
12. Rao, H.; Narayanappa, P.; Rao, L.; Shivapuji, A. M.; Dasappa, S.; Plasma activated water generation, characterization and application for seed germination and plant growth; in *Proceedings of ISPC,* **2019**, *24*.
13. Narayanappa, P.; Singh, A.; Rao, L.; Dasappa, S.; Decentralized Grey Water Recovery System Using Cold Plasma for Rural India. *Proc. ISPC,* **2017**, *23*.
14. Kumar, Amit; Anand M. S.; Rao, L.; D. S.; Cold Plasma Methane Reforming; in 11th Asia Pacific Conference on Combustion **2017**.
15. Kamgang-Youbi, G.;; Herry, J. M.; Meylheuc, T.; Laminsi, S.; Naïtali, M.; *J. Chem. Technol. Biotechnol.,* **2018**, *93,* 2544.
16. Lukes, P.; Dolezalova, E.; Sisrova, I.; Clupek, M.; *Plasma Sources Sci. Technol.,* **2014**, *23*.
17. Thirumdas, R.; *et al.; Trends Food Sci. Technol.* **2018**, *77,* 21.
18. Zimmermann, J. L.; *et al.; J. Phys. D. Appl. Phys.,* **2011**, 44.
19. Boxhammer, V. *et al.; New J. Phys.,* **2012**, *14,* 113042.
20. Li, Y. F.; Shimizu, T.; Zimmermann, J. L.; Morfill, G. E.; *Plasma Process. Polym.,* **2012**, *9,* 585.
21. Pompl, R. *et al.; New J. Phys.,* **2009**, *11*.
22. Kvam, E.; Davis, B.; Mondello, F.; Garner, A. L.; *Antimicrob. Agents Chemother.,* **2012**, *56,* 2028.
23. Fridman, G. *et al.; Plasma Chem. Plasma Process.,* **2007**, *27,* 163.
24. Kuo, M. T.; *Antioxid. Redox Signal.,* **2008**, *11,* 99.
25. Laurita, R.; Barbieri, D.; Gherardi, M.; Colombo, V.; Lukes, P.; *Clin. Plasma Med.,* **2015**, *3,* 53.
26. Zhang, J.; Studies, A.; Arar, E. J.; Agency, U. S. E. P.; Determination of Nitrate and Nitrite in Estuarine and Coastal Waters by Gas Segmented Continuous Flow Colorimetric Analysis School of Marine and Atmospheric Science / AOML, NOAA, University of Miami, Miami, Peter B. Ortner and Charles J . Fischer, O. *ReVision,* **1997**, 1.
27. Sreekumar, N. V.; Narayana, B.; Hegde, P.; Manjunatha, B. R.; Sarojini, B. K.; *Microchem. J.,* **2003**, *74,* 27.
28. Shen, J. *et al.; Sci. Rep.,* **2016**, *6*.
29. Naítali, M.; Kamgang-Youbi, G.; Herry, J. M.; Bellon-Fontaine, M. N.; Brisset, J. L.; *Appl. Environ. Microbiol.,* **2010**, *76,* 7662.
30. Vlad, I. E.; Anghel, S. D.; *J. Electrostat.,* **2017**, *87,* 284.
31. Judée, F.; Simon, S.; Bailly, C.; Dufour, T.; *Water Res.,* **2018**, *133,* 47.
32. Xiang, Q. *et al.; LWT,* **2018**, *96,* 395.
33. Chauvin, J.; Judée, F.; Yousfi, M.; Vicendo, P.; Merbahi, N.; *Sci. Rep.,* **2017**, *7,* 1.
34. Gaydon, A. G.; The Identification of Molecular Spectra; Springer Netherlands, **1976**.
35. Chen, Z. *et al.;* Selective Treatment of Pancreatic Cancer Cells by Plasma-Activated Saline Solutions; IEEE Trans. Radiat. Plasma Med. Sci., **2017**, *2,* 116.
36. Connor, N. O.; Humphreys, H. H.; Daniels, S.; Oxygen line ratio method for the determination of plasma parameters in atmospheric pressure discharges using air as the working gas. *31st ICPIG,* 2013, *2*.